Prediction of Stress–Relaxation and Creep of Linear Aromatic Polyesters Related to Poly(ethylene Terephthalate) in the Nonlinear Range*

TIE HWEE NG† and H. LEVERNE WILLIAMS, *Department of Chemical Engineering and Applied Chemistry, University of Toronto, Toronto, Ontario, Canada M5S 1A4*

Synopsis

A study of the nonlinear viscoelastic properties of polymers was made using the Halsey-Eyring model with one- and three-dimensional mathematical analyses. Various parameters to calculate stress–relaxation and creep could be calculated from a single stress–strain curve of the same polymer. The parameters so calculated reconstituted the stress-strain curves, the one-dimensional equations yielding the better fit. The same constants were applied to predict stress-relaxation and creep. The fit using the three-dimensional equations is much better for stress-relaxation and creep than the one-dimensional equations.

INTRODUCTION

Linear viscoelastic properties of solid polymers have been studied extensively both experimentally and theoretically. In use, polymeric materials may be subjected to deformations beyond the linear viscoelastic region and this has prompted some theoretical and experimental studies into the nonlinear range. Eyring and Halsey[1–3] developed a set of one-dimensional constitutive equations based on a model composed of two springs and a nonlinear dashpot. Eyring[4] also drew attention to the relationship of the viscosity of the dashpot to the rate of strain.

These concepts were applied by Haward and Thackray[5] to establish empirical constitutive equations for the one-dimensional treatment of the three-element model with the viscosity varying with the rate of strain; a Hookean spring in series with a Voigt unit, the combination of an Eyring dashpot parallel to a rubber elasticity spring. Titomanlio and Rizzo[6,7] extended the concepts to a three-dimensional treatment using the equivalent model of a linear spring parallel to a Maxwell unit composed of a dashpot and a second spring. The viscosity of the dashpot was allowed to change with the rate of strain by an Eyring-type mechanism and the effects of free volume changes were included by use of the Doolittle[8] equation.

*Presented in part at the 28th IUPAC Macromolecular Symposium, Amherst, MA, July 12–16 (1982), the 22nd Canadian High Polymer Forum, Waterloo, Ont. Aug 10–12 (1983), and the Canadian Society for Chemical Engineering, 33rd Conference, Toronto, Ont., Oct. 2–5 (1983).

†Present address: Xerox Research Centre of Canada Ltd., Mississauga, Ontario.

Journal of Applied Polymer Science, Vol. 33, 739–757 (1987)

CCC 0021-8995/87/030739-19$04.00

TABLE I
Parameters Used to Predict the Viscoelastic Behavior of Polyester Samples, $\dot{\epsilon} = 6.67\ h^{-1}$ [12]

	One-dimensional					Three-dimensional			
Polyester[a]	E_1 MPa	E_2 MPa	K s^{-1}	β	V_h Å^3	B 10^{-1} MPa^{-1}	R 10^{-2} Pa^{-1}	G_1 MPa	G_2 MPa
4GT	1600	79.5	1.0×10^{-4}	18.70	6.5×10^2	2.72	0.7	472	70
6GT	700	56.8	5.7×10^{-4}	3.28	8.0×10^2	7.97	1.7	185	58
8GT	425	42.7	4.7×10^{-4}	3.92	9.5×10^2	11.59	2.5	80	60
10GT	320	83.3	3.2×10^{-4}	5.89	1.3×10^3	13.28	3.0	111	15
4GI	940	56.0	1.5×10^{-3}	1.25	2.3×10^2	4.23[b]	1.1	232	30
6GI	320	8.7	5.6×10^{-4}	3.33	1.0×10^3	11.17	2.6	74	21
8GI	140	47.8	3.5×10^{-5}	52.36	7.2×10^3	21.56[b]	5.0	35	28
10GI	98	2.0	5.2×10^{-6}	360.00	2.3×10^4	54.72	12.0	32	14
3GTcoI	350	24.2	8.4×10^{-3}	0.22	1.2×10^2	8.39	2.0	93	7
4GTcoI	340	21.2	2.6×10^{-4}	7.03	1.3×10^2	6.46	1.6	116	4
6GTcoI	38	4.0	4.2×10^{-4}	4.40	5.2×10^3	31.45	7.5	10	1
10GTcoI	114	13.0	41.7×10^{-3}	4.44	2.7×10^3	24.06	7.0	29	13

[a] For significance of codes see Experimental.
[b] Rest relaxation time = 1 year.

However, their constitutive equations do not seem to have been extended to stress relaxation or creep. A revised three-dimensional treatment has been devised which uses a different three-dimensional Maxwell equation suggested by Oldroyd,[9] a variable viscosity function, and the imposition of constraints in the evaluation of the parameters.[10]

Three series of linear aromatic polyesters had been synthesized.[11] These formed series of polymers differing in known ways. It was of interest to study their time-dependent mechanical behavior at large deformations, to describe other nonlinear viscoelastic features of a mechanical model whose constant parameters could be evaluated from the stress-strain data, and to correlate these parameters with the structures of the polyesters which had known chain configurations.

To test the validity of the concepts the stress-strain data for three series of aromatic polyesters were used to calculate the necessary constants[12] for both the one-dimensional and three-dimensional treatments (Table I). The constants were then used to reconstitute the stress-strain curves and it was found that the one-dimensional equations yielded a somewhat better fit than did the three-dimensional. The same constants are now used to predict the stress-relaxation and creep curves. These are compared to the experimental data.

THEORY

The mathematical derivation of the constitutive equations may be found in the complete work.[10] The one-dimensional equations for the model, illustrated by two Hookean springs and an Eyring nonlinear dashpot are:[5]

$$\sigma = \sigma_1 + \sigma_2, \tag{1}$$

$$\frac{d\sigma_1}{dt} + E_1 K \sinh\left(\frac{V_h \sigma_1}{2kT}\right) = E_1 \frac{d\epsilon}{dt}, \tag{2}$$

and

$$\sigma_2 = E_2\epsilon. \tag{3}$$

in which σ is the tensile stress, ϵ is the tensile strain, and E_1 and E_2 are the tensile moduli of the springs. The expression

$$K \sinh\left(\frac{V_h\sigma_1}{2kT}\right) \tag{4}$$

is equal to the rate of strain of the dashpot.[13,14] V_h is the Eyring activation volume, k is Boltzmann's constant, T is absolute temperature and K is a constant.

The three-dimensional constitutive equations for the model of a Maxwell element parallel to a rubber-like spring are:[6,7]

$$\boldsymbol{\sigma} = \boldsymbol{\sigma}_1 + \boldsymbol{\sigma}_2, \tag{5}$$

$$\boldsymbol{\sigma}_1 + \lambda\dot{\boldsymbol{\sigma}}_1 = 2\eta\mathbf{d}, \quad \text{and} \tag{6}$$

$$\boldsymbol{\sigma}_2 = 2G_2\dot{\mathbf{L}}_G. \tag{7}$$

Tensile stress $\boldsymbol{\sigma}$ and the Lagrangian finite strain $\mathbf{L}_G$ are represented by their respective tensors of second order. λ is the relaxation time given by η/G_1. G_2 and G_1 are the shear moduli of the Maxwell spring and the rubber elasticity spring respectively. η is the viscosity of the dashpot and $\mathbf{d}$ is the rate of deformation tensor.

The time derivative of tensile stress $\dot{\boldsymbol{\sigma}}_1$ is:

$$\frac{\mathscr{D}\boldsymbol{\sigma}_1}{\mathscr{D}t} + a\{\boldsymbol{\sigma}_1 \cdot \mathbf{d} + \mathbf{d} \cdot \boldsymbol{\sigma}_1\} \tag{8}$$

in which a is a constant and $\mathscr{D}/\mathscr{D}t$ is the corotational or Jaumann derivative.

A variable viscosity is used and is expressed similarly to Titomanlio and Rizzo[6] who included the Eyring viscosity equation and the Doolittle free volume effect. The equation was changed by including $|\tau_1|$, the magnitude of the deviatoric stress tensor,[15] as follows:

$$\eta\alpha|\tau_1|\exp\left(\frac{40}{1 + R(\boldsymbol{\sigma}_1 : \boldsymbol{\delta})} - B|\tau_1|\right) \tag{9}$$

A rest relaxation time of 20 years is used, R and B are constants with the dimensions of Pa^{-1}, and $(\boldsymbol{\sigma}_1 : \boldsymbol{\delta})$ is the first invariant of the stress tensor.[16]

The first constraint applied in the calculations is that $E_{sec}/3 > G_2$ which guarantees stress-relaxation rather than stress-growth with time. (E_{sec} is the secant tensile modulus.) The second is that $G_2 > E_2/3$ where E_2 is a modulus as used in the stress-strain equation.[12] This second constraint arises from the relationships:

$$\frac{d\sigma}{d\epsilon} = 2G_2(1 + \epsilon) = E_2 \tag{10}$$

so that a constraint on ϵ of 0.5 is used. The third constraint is that $40 < B/R < 100$ which assures that the ratio B/R is in a realistic range such that the free volume effect and the Eyring effect on the viscosity of the dashpot are equally important.

In a stress-relaxation test when the strain ϵ is held constant at ϵ_0, the one-dimensional equation is:

$$\sigma(t) = \frac{2}{\phi}\tanh^{-1}\left\{\tanh\left[\frac{\phi(\sigma_0 - E_2\epsilon_0)}{2}\right]\exp(-KE_1\phi t)\right\} + E_2\epsilon_0 \qquad (11)$$

where ϕ, E_2, K, and E_1 are all functions of a constant β which was predetermined by data fitting of the stress-strain curves using the one-dimensional approach as discussed earlier.[12] σ_0 is the stress at time zero. Similarly, the three-dimensional equations give:

$$\frac{d\sigma}{dt} = \frac{G_2 h - \sigma}{F\left(1 + \frac{|\tau_1|}{G_1}\right)\exp\left(\frac{40}{1 + R(\sigma:\delta)} - B|\tau_1|\right)} \qquad (12)$$

where $h = \dfrac{(1-\epsilon_0)^3 - 1}{1 + \epsilon_0}$, (13)

$$|\tau_1| = \frac{\sqrt{6}}{3}(\sigma - G_2 h), \qquad (14)$$

$$(\sigma_1 : \delta) = \sigma - G_2\left[\frac{3\epsilon_0^3 + \epsilon_0^3}{1 + \epsilon_0}\right], \quad \text{and} \qquad (15)$$

$$F = \lambda_0 \exp(-40). \qquad (16)$$

Equation (12) is a nonlinear differential equation. It cannot be solved analytically, and recourse must necessarily be made to numerical methods. One of these is the Runge-Kutta method of order 4 which was employed here to estimate the stress-relaxation behavior of the various polyesters. Based on the parameters previously determined[12] any stress–relaxation curve can be calculated once the initial conditions σ_0 and ϵ_0 are specified.

In a creep test where the load is held constant at σ_0, the one-dimensional equation is given as follows:

$$\sigma_0 = \frac{\sigma_0}{E_2} - \frac{2}{\phi E_2}\tanh^{-1}\left\{\tanh\left[\frac{\phi(\sigma_0 - \epsilon_0 E_2)}{2}\right]\exp\left[-k\phi\frac{E_1 E_2}{E_1 + E_2}t\right]\right\} \qquad (17)$$

where E_1, E_2, K, and ϕ are the constant parameters previously determined.[12]

Similarly, for the three-dimensional analysis, the creep equation is given by:

$$\frac{d\epsilon}{dt} = \frac{\sigma_0(1+\epsilon) - G_2\left[(1+\epsilon)^3 - 1\right]}{\lambda\left[3(G_1+G_2) + G_2(1+a)\left(\frac{1}{1+\epsilon} + 2\epsilon^2 + 4\epsilon - 1\right) - 2a\sigma_0\right]} \tag{18}$$

$$\text{where } \lambda = \lambda_0\left(1 + \frac{|\tau|}{G_1}\right)\exp\left[-40 + \frac{40}{1 + h(\sigma_1 : \delta)} - B|\tau|\right] \tag{19}$$

The initial condition is that at $t = 0$, $\epsilon(0) = \epsilon$.

Similarly to the stress-relaxation equation, Eq. (18) above is a nonlinear differential equation. The Runge-Kutta method of order 4 was used to solve for the strain ϵ with respect to time t. The same parameters previously determined from a single stress-strain curve are substituted into Eq. (18) to calculate the total strain ϵ. The initial strain ϵ_0 is then subtracted from the total strain ϵ to obtain the subsequent strain $\Delta\ell_s/\ell_o$ right after time zero of a creep test. The quantity $\Delta\ell_s$ is the subsequent elongation of the specimen during the creep experiment. Unlike the stress-relaxation equation, the creep equation contains the constant a since it is related to the rate of deformation tensor **d**.

EXPERIMENTAL

Chemicals and polymerization technique for the linear aromatic polyesters used in this work were described previously.[11] The chemical structures are indicated by a code of letters following a number. The number indicates the number of methylene groups in the glycol, *n*G. T, I and TcoI indicate the terephthalate, isophthalate, and copolymer series, respectively. The well known Dacron would be 2GT.

Film samples of all *n*GT, as well as 3GI and 4GI were prepared by a hot-pressing technique using a laboratory press at about 10 K above the melting temperature for 3 min, giving a film thickness of about 0.3 mm and a diameter of about 20 cm. The samples were then removed from the hot press and cooled to room temperature. Solution-cast films were obtained for 6GI, 8GI, 10GI, 3GTcoI, 4GTcoI, 6GTcoI and 10GTcoI by pouring an approximately 10% solution in dichloromethane onto a glass plate floating on mercury and then drying gradually at room temperature for two days. The samples were then dried in a vacuum oven at 313 K for 1 day before storing in a desiccator until used.

All samples were cut in the same direction (e.g., in the radial direction of the circular sheet) into standard shaped dumbbell pieces. The mean effective length (ℓ_e) of the experimental samples was determined using the technique outlined by Titomanlio and Rizzo.[17] Basically, two lines 3 cm apart were marked at the central portion of the specimen. The samples were elongated in an Instron tensile testing machine at a crosshead speed of 0.5 cm · min^{-1}. The machine crosshead was stopped when the yield point was reached. The ratios of the displacements between the two lines and the two jaws of the testing machine were determined and a mean value of the ratio was calculated. The

number three divided by the ratio gave the mean effective length of the sample in centimeters. Subsequently, all strains ϵ were determined using the expression $\epsilon = \Delta\ell/\ell_e$ where ℓ_e was found to be 4.5 ± 0.3 cm and $\Delta\ell$ is the displacement of the Instron jaws.

The experimental results of load versus elongation were converted into true-stress versus strain, where the true-stress is equal to $(1 + \epsilon)$ times the engineering stress, by assuming a constant density.

The tensile elongation tests were performed at room temperature (295 K) by means of an Instron Universal Testing Instrument, floor model TT. Two

TABLE II
Strain History of Specimens Subjected to a Constant Strain Rate $\dot{\epsilon} = 6.67\ h^{-1}$ Prior to a Stress-Relaxation Test

Polyester	σ_0 (MPa)	ϵ_0	t* (s)
4GT	49.1	0.061	33
	43.4	0.036	19
	35.7	0.025	13
6GT	24.7	0.097	53
	22.5	0.061	33
8GT	21.8	0.090	49
	19.6	0.069	37
	16.3	0.050	27
	8.5	0.020	11
10GT	21.8	0.088	47
	20.2	0.075	41
	18.2	0.064	35
4GI	31.2	0.104	56
	27.2	0.064	35
	21.1	0.036	19
6GI	15.2	0.160	86
	14.8	0.103	56
	11.7	0.055	30
8GI	4.2	0.023	12
	3.4	0.019	10
10GI	2.9	0.172	93
3GTcoI	21.0	0.378	204
	17.3	0.185	100
	14.8	0.120	65
4GTcoI	28.8	0.716	386
	23.8	0.467	252
	18.2	0.240	130
6GTcoI	7.5	1.10	594
	6.1	0.72	389
	5.2	0.49	264
	4.8	0.40	216
10GTcoI	8.7	0.148	80
	5.8	0.103	56
	7.7	0.062	33
	3.7	0.033	18
	8.7	0.148	80
	5.8	0.103	56
	7.7	0.062	33
	3.7	0.033	18

elongation rates, 0.5 cm · min^{-1} and 2.0 cm · min^{-1}, were chosen. During elongation, samples were inspected visually to ensure that the deformation was homogeneous throughout the constant cross-sectional region of the test piece. The sample was strained until fracture or the first sign of necking. The stress-strain curves of the samples cut from the same sheet of film showed very good reproducibility with less than four percent standard deviation. Specimens of the same polyester prepared from two different sheets of film showed a slightly higher standard deviation of approximately 7 percent.

The stress-relaxation experiments were carried out at 295 K on the Instron. First the specimen was loaded at a constant strain rate $\dot{\epsilon} = 6.67\ h^{-1}$ for a duration t^* to the initial stress σ_0 and the initial strain ϵ_0. The strain history prior to the stress relaxation tests is given in Table II. After straining was stopped instantaneously, the stress relaxation at constant ϵ_0 began. Two or three stress-relaxation curves of the same material were obtained at different strain levels usually beyond the yield point but below the strain levels where necking started to occur. Each test lasted for about 24 h. Care was taken to apply uniform pressure on the two jaws to keep plastic deformation of the material inside the jaws as small as possible during stress-relaxation.

The creep tests were performed also on the Instron Testing Instrument with the aid of a duPont 943 Thermomechanical Analyzer (TMA). The heart of the 943 TMA is a movable-core linear variable differential transformer (LVDT). The position of the core, which was connected to the probe, determines the voltage induced in the transformer secondary windings. This voltage is applied to the vertical axis of the duPont 990 x-y recorder. The TMA is capable of measuring a displacement as small as 0.5 μm per cm of chart.

For a creep test, a sample was deformed at a constant strain rate $\dot{\epsilon} = 6.67\ h^{-1}$ to some value of the force which was then held constant. The constant stress σ_0, initial strain ϵ_0 and the length of time t^* experienced by the specimens at the rate $\dot{\epsilon} = 6.67\ h^{-1}$ prior to each creep test are given in Table III. The subsequent displacement $\Delta\ell_s$ of the lower jaws was measured by

TABLE III
Strain History of Specimens Subjected to a Constant Strain-Rate $\dot{\epsilon} = 6.67\ h^{-1}$ Prior to a Creep Test

Polyester	σ_0 (MPA)	ϵ_0	t* (s)
4GT	50.2	0.070	38
6GT	22.3	0.060	32
8GT	20.9	0.080	43
10GT	18.8	0.065	35
4GI	27.0	0.062	33
6GI	14.7	0.100	54
10GI	2.9	0.170	92
3GTcoI	17.1	0.189	102
4GTcoI	18.1	0.230	124
6GTcoI	4.8	0.390	210
10GTcoI	3.7	0.034	18
10GTcoI	7.7	0.102	55
10GTcoI	8.7	0.145	78

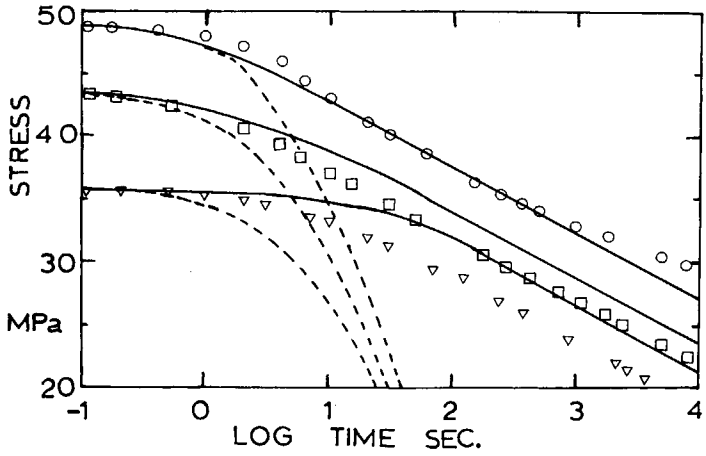

Fig. 1. Stress-relaxation data for 4GT at initial stress (○) 49.1 MPa, (□) 43.4 MPa, and (▽) 35.7 MPa. Dashed lines, calculated for one-dimensional, solid lines for three-dimensional approach. (Parameters from Table I.)

means of the TMA. As the sample deformed under the load, a rigid steel bar attached to the crosshead of the Instron moved the probe of the TMA in the same direction. The movement of the probe with respect to an original reference point on the LVDT was recorded on the duPont 990 plotter. The TMA could only detect the displacement of the probe from the original reference point up to a maximum distance of 0.375 cm. Before the maximum displacement was reached, the LVDT was readjusted to set a new zero reference point such that a further elongation of 0.375 cm could be measured. This process was repeated as often as required during a creep test of approximately 5 h.

RESULTS AND DISCUSSION

Prediction of Stress-Relaxation

Figures 1 through 5 compare some of the predictions of stress-relaxation with the experimental results obtained on twelve different polyesters. Figure 1 shows the stress-relaxation curves of 4GT at three different strain levels, all in the nonlinear viscoelastic region. The one-dimensional calculations yield very unrealistic predictions of the stress-relaxation behavior. In less than 70 s of decay time, all stresses had relaxed to below 20 MPa. The three-dimensional prediction shows reasonable agreement with the experimental data. The discrepancies between the experimental and theoretical values increase slightly at lower initial stresses σ_0. Good agreement of the stress-relaxation data for 6GT with those predicted by the three-dimensional approach was likewise obtained.

In Figure 2, the three-dimensional theoretical predictions of stress-relaxation based on two different variable viscosity functions are compared for 8GT. Both predictions are regarded as fair. With $\eta\alpha|\tau_1|\exp(-B|\tau_1|)$ a slower rate of stress-relaxation is predicted than with $\eta\alpha\exp(-B|\tau_1|)$. The former suggests a higher viscosity and hence a longer relaxation time. It is difficult to judge which viscosity function will make a better model prediction in general. A

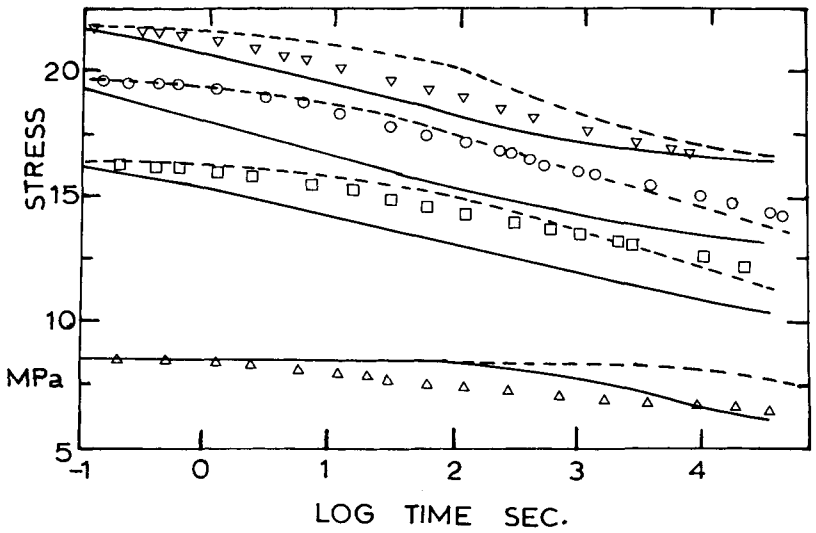

Fig. 2. Stress-relaxation data for 8GT at initial stress (▽) 21.8 MPa, (○) 19.8 MPa, (□) 16.3 MPa, and (△) 8.5 MPa. Dashed lines were calculated for three-dimensional equations using $\eta\alpha|\tau_1|\exp(-B|\tau_1|)$ and solid lines were calculated using $\eta\alpha\exp(-B|\tau_1|)$. (Parameters from Table I.)

guideline is that the former viscosity function may be used where stress-relaxation is carried out at high strain levels while the latter function may be better at lower strain levels.

The predictions by both models for 10GT were regarded as poor. However, the one-dimensional treatment showed a more favorable performance here than it did anywhere else. The graphical determination of the modulus E_2 from the stress-strain curve of 10GT was subjective since a straight line portion beyond the yield point did not exist. This in turn makes the evaluation of the shear modulus G_2 difficult. Besides, experimental data of 10GT showed a very rapid rate of stress-relaxation. In less than 1 h, the material had relaxed to about 40% of its initial stress. A rest relaxation time τ_0 of 1 day was chosen for this analysis. The three-dimensional analysis predicted a slower rate of relaxation, however. At long times, the measured values of the stress seem to reduce asymptotically to the same value, 5 MPa. The one-dimensional data reached asymptotic values higher than those of the experimental in about 600 s.

Generally fair agreement between the three-dimensional predictions and the experimental stress-relaxation curves of 4GI and 6GI at various strain levels were obtained. In Figure 3 the stress-relaxation curves of 8GI show that the material broke at a relaxation duration of around 200 s. Careful examination of the failed samples revealed the existence of cracks and microvoids. Repetition of the test with specimens cut from the same sheet showed reproducible data. To allow for this early failure, a rest relaxation time τ_0 of 1 year was chosen. The results of the three-dimensional predictions proved to be unrealistic. The one-dimensional approach with a much faster rate of stress decay gives slightly better predictions. Similar data showed that the stress-relaxation of 10GI agreed fairly well with the three-dimensional predictions.

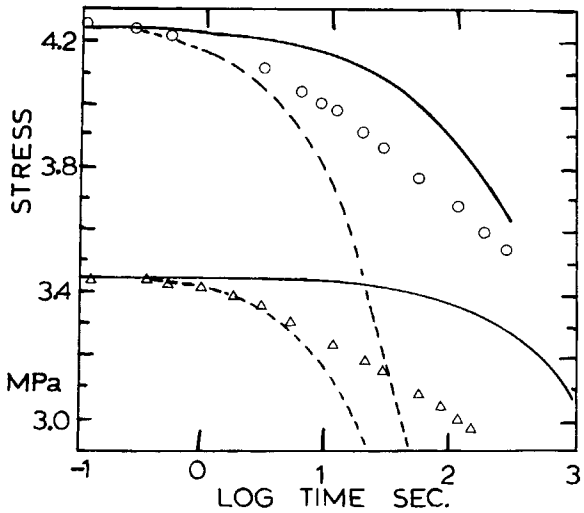

Fig. 3. Stress-relaxation data for 8GI at initial stress (○) 4.23 MPa and (△) 3.45 MPa. Dashed curves calculated for one-dimensional, solid curves for three-dimensional equations. (Parameters from Table I.)

The experimental relaxation curves of 3GTcoI approached each other at longer times, whereas the theoretical curves based on the three-dimensional analysis did not. All three curves were tested above the yield stress. The plots for 4GTcoI were again in good agreement with predictions. Figure 4 for 6GTcoI again showed fair agreement of the data with theoretical by the three-dimensional equations.

Figure 5 shows the remarkable resemblance of the relaxation behavior of 10GTcoI to those of 8GT given in Figure 2 except that the former was carried out at lower values of σ_0.

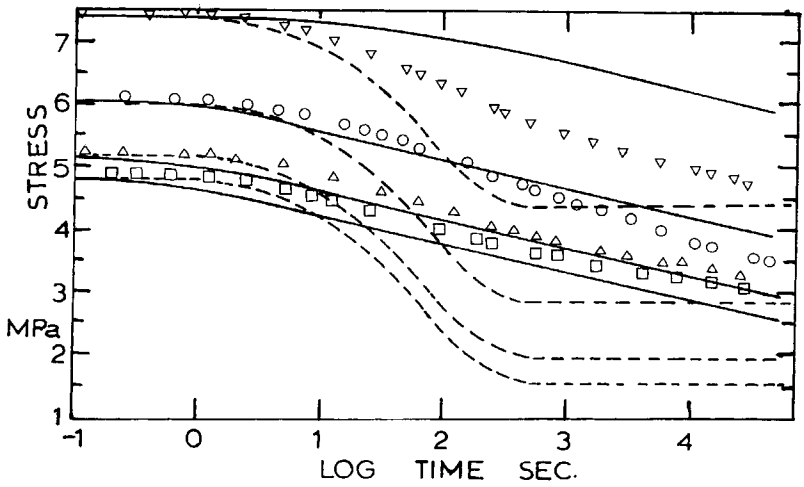

Fig. 4. Stress-relaxation data for 6GTcoI at initial stress (▽) 7.5 MPa (○) 6.1 MPa, (△) 5.2 MPa and (□) 4.8 MPa. Dashed lines are calculated for one-dimensional, solid lines for three-dimensional equations. (Parameters from Table I.)

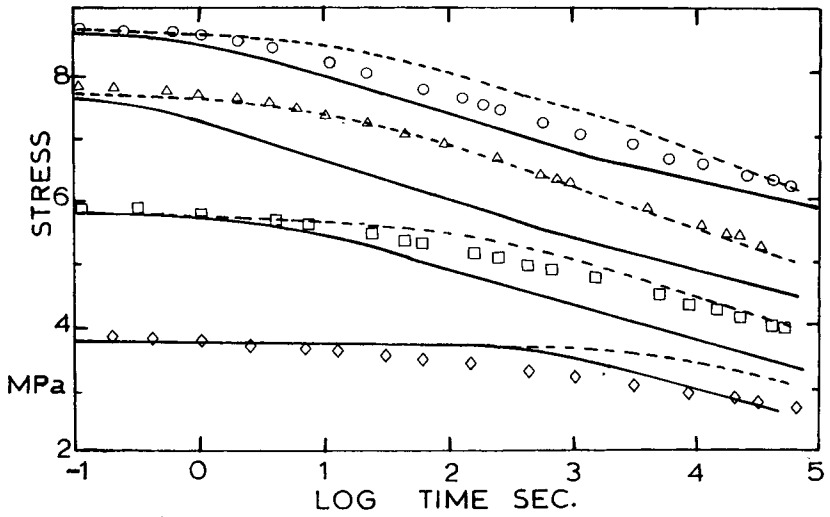

Fig. 5. Stress-relaxation data for 10GTcoI at initial stress (○) 8.7 Mpa, (△) 7.7 Mpa, (□) 5.8 MPa, and (◇) 3.7 MPa. Dashed lines calculated for three-dimensional system using $\eta\alpha|\tau_1|\exp(-B|\tau_1|)$ and solid lines for same using $\eta\alpha\exp(-B|\tau_1|)$. (Parameters from Table I.)

In order to compare the relaxation rates of each series of polyesters and at different constant strain levels, the percent stress relaxation defined as $[\sigma_0 - \sigma(t)]/\sigma_0 \times 100\%$, was plotted against time as shown in Figures 6, 7, and 8. The corresponding values of the constant strain ϵ_0 are shown in Table II.

Figure 6 shows that the percent stress-relaxation with time of 8GT beyond the yield point is completely independent of the constant strain level. The curves for 6GT are nearly parallel indicating the same rate of relaxation at the

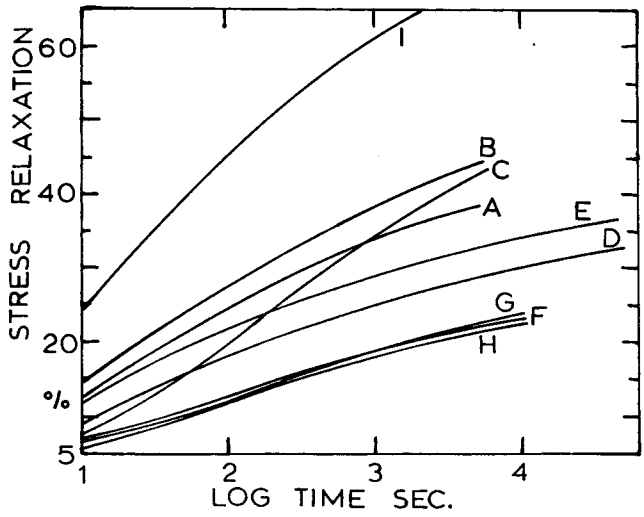

Fig. 6. Percent stress-relaxation versus time for the terephthalate series. 4GT at initial stress (A) 49.1 MPa, (B) 43.1 MPa, and (C) 35.7 MPa; 6GT at initial stress (D) 24.7 MPa and (E) 22.5 MPa; 8GT at initial stress (F) 21.8 MPa, (G) 19.6 MPa, and H 16.3 MPa; and 10GT at initial stress (I) 21.8 MPa.

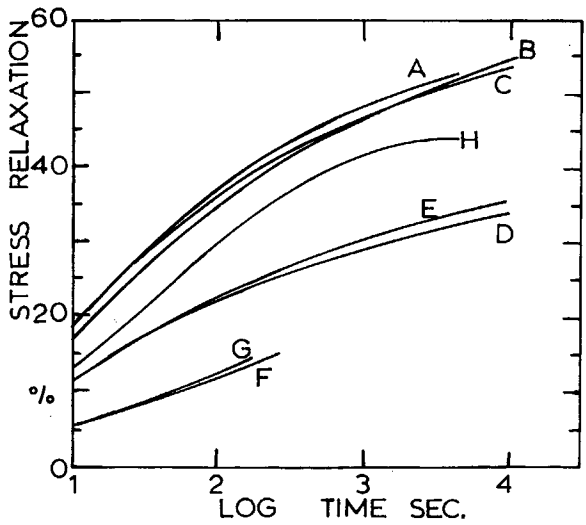

Fig. 7. Percent stress-relaxation versus time for the isophthalate series 4GI initial stress (A) 31.2 MPa, (B) 27.2 MPa, and (C) 21.2 MPa; 6GI at initial stress (D) 14.8 MPa and (E) 11.7 MPa; 8GI at initial stress (F) 4.23 MPa and (G) 3.45 MPa; and 10GI at initial stress (H) 2.9 MPa.

two different strain levels. There is no definite trend for the curves of 4GT. This behavior might be attributed to the fact that the experimental curves were obtained for different viscoelastic regions. One was stress-relaxed at the beginning of the neo-Hookean region ($\epsilon_0 = 0.025$); the second was observed at the transition of the yield point ($\epsilon_0 = 0.036$), while the third was obtained beyond the yield point ($\epsilon_0 = 0.061$). The curve for 10GT demonstrates a rapid rate of relaxation. Within 1 h, only about 30% of its original stress remained. It is plausible that there was less hindrance to the rearrangement and less friction of the segments making up the macromolecular structure thereby facilitating the viscous flow. Except for 10GT, the percent stress relaxation at a given time for the terephthalate series decreases with increasing number of (CH_2) groups.

Figure 7 shows the dependence of the percent stress-relaxation with time for the isophthalate series. The curves of the three samples, 4GI, 6GI and 8GI, show independence of the constant strain level. Similar to the terephthalate series, the percent stress relaxation at a given time increases with decreasing number of (CH_2) groups except that for 10GI. Figure 8 shows the percent stress-relaxation with time for the copolyester series. The curves for 6GTcoI show complete independence of the strain level below 400 s.

It should be noted that all stress-relaxation experiments were carried out after a short duration time of extension. The experimental time was measured from the time when the extension stopped and the relaxation began. According to the Boltzmann superposition principle in the linear viscoelastic theory, the time should be measured from the beginning of the extension.[18,19] However, the small difference in the reference zero time affects very little the long time behavior. The relaxation stress $\sigma(t)$ measured after the specimen is subjected to a constant rate of strain for a short time is expected to be less than that obtained in a classical method where a finite strain is applied

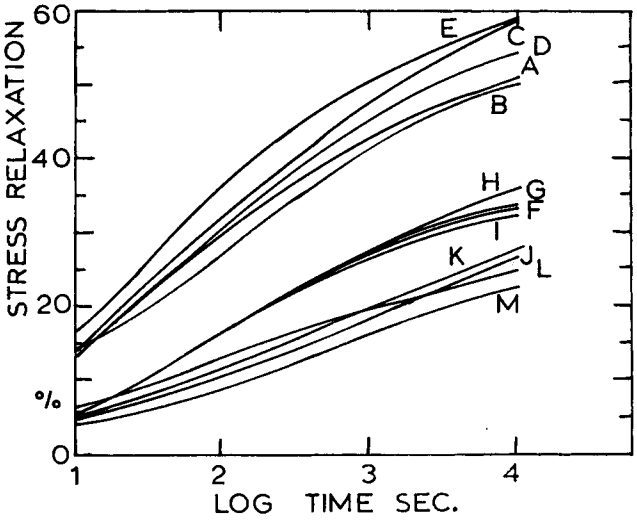

Fig. 8. Percent stress-relaxation versus time for copolyester series. 3GTcoI at initial stress (A) 21.0 MPa and (B) 17.3 MPa; 4GTcoI at initial stress (C) 28.8 MPa, (D) 23.8 MPa, and (E) 18.2 MPa; 6GTcoI at initial stress (F) 7.5 MPa, (G) 6.1 MPa, (H) 5.2 MPa, and (I) 4.8 MPa; and 10GTcoI at initial stress (J) 8.7 MPa, (K) 7.7 MPa, (L) 5.8 MPa, and (M) 3.7 MPa.

instantaneously. In the former case, a substantial amount of stress-relaxation has taken place during the short loading time.

The stress-relaxation data on 6GTcoI were selected for a more detailed analysis because the strain level covers a wider range of interest (from 0.4 to 1.09). Figure 9 shows the ratio of time-dependent tensile stress to tensile strain plotted logarithmically against time at different strains for 6GTcoI. The results demonstrate a nonlinear stress-relaxation behavior because four differ-

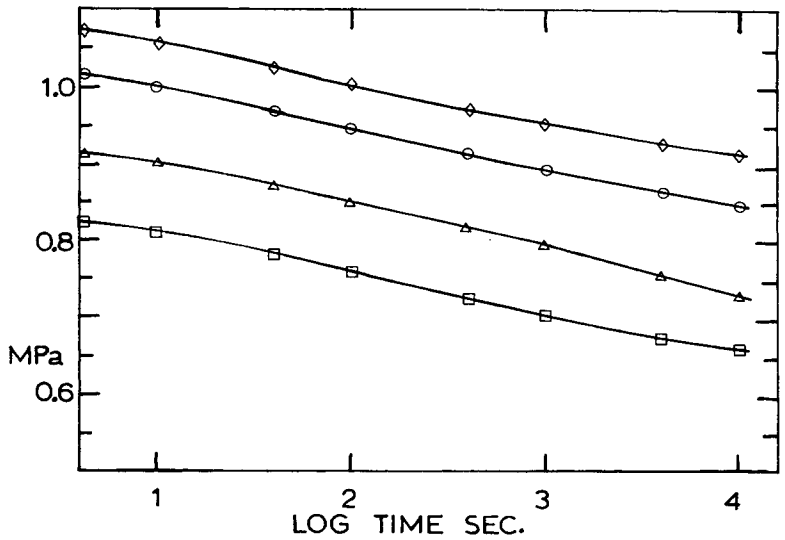

Fig. 9. Tensile stress-relaxation of 6GTcoI at constant strains of (◇) 0.40, (○) 0.49, (△) 0.72, and (□) 1.09.

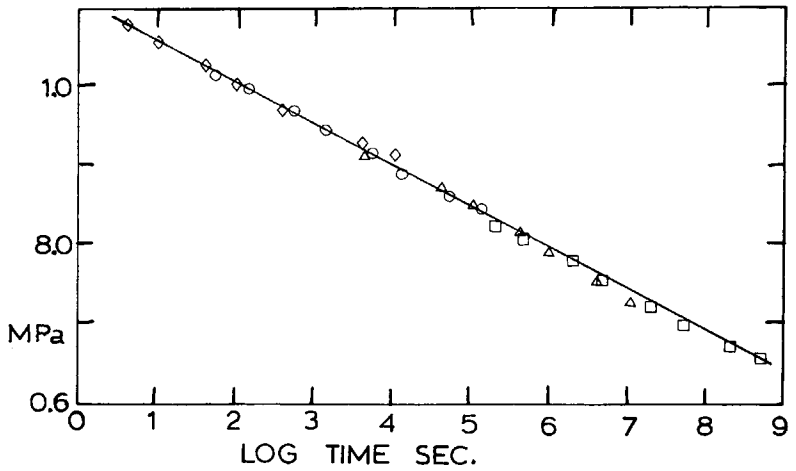

Fig. 10. Composite curve for the ratio of time-dependent tensile stress to tensile strain of 6GTcoI by plotting the data of Fig. 9 to a reference strain of 0.4.

ent curves were obtained. The differences can be interpreted as due to a decrease in the viscosity or relaxation time[20] with increasing stress. These different curves can be combined into a composite curve by means of a shift factor a_s as shown in Figure 10. The corresponding shift factor a_s shown in Figure 11 demonstrates that it is a strongly decreasing function of strain. It is doubtful, however, whether a_s can be entirely related to fractional free volume in semicrystalline polymers[20] as it is for amorphous polymers.

Published data[21] on the stress-relaxation of HDPE were studied also. The stress-strain data on HDPE at $\dot{\epsilon} = 1.3 \times 10^{-3}$ s^{-1} were selected because the strain rate is closest to that used for the polyesters which was $\dot{\epsilon} = 1.85 \times 10^{-3}$ s^{-1}. These data were replotted together with those of 6GT and 8GT in Figure 12. The stress-relaxation data of HDPE at room temperature, with different

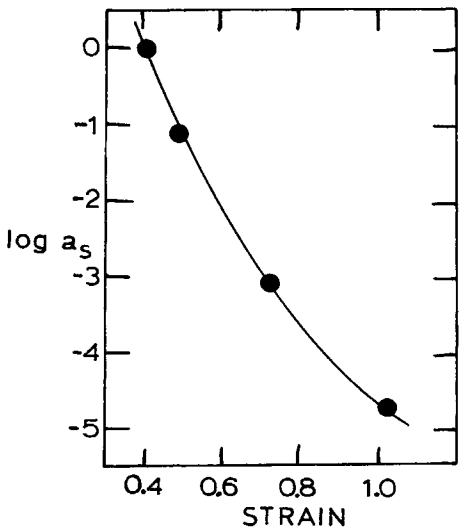

Fig. 11. Shift factors used in plotting Fig. 10.

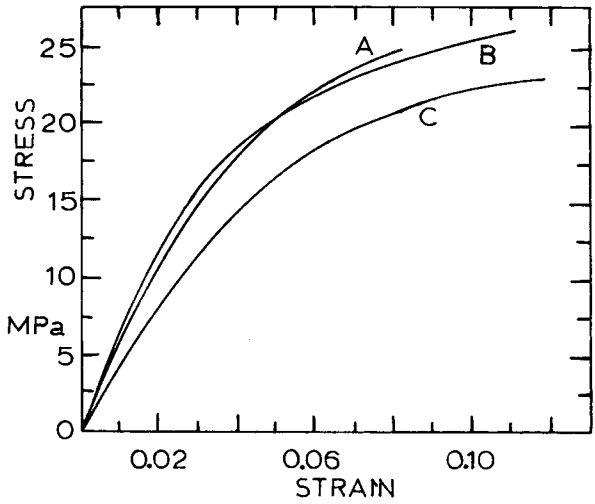

Fig. 12. Stress-strain data for (A) high-density polyethylene at a strain rate of 1.3×10^{-3} s^{-1} replotted from Shinozaki and Sargent.[21] Data for (B) 6GT and (C) 8GT replotted from Fig. 1, Ref. 12.

initial stretching histories as given in the legend, are in Figure 13. In order to predict the stress-relaxation behavior of HDPE using the three-dimensional equations, it was assumed that it behaved very much like 7GT as demonstrated by the fact that most of the stress-strain curve for HDPE lies between those for 6GT and 8GT. Therefore, $n = 7$ was substituted into Eqs. (5) to (7) to obtain the three-dimensional parameters G_1, G_2, R, and B. These values are given in the caption of Figure 13. The three-dimensional predictions are shown in Figure 13. The main features of the theoretical stress-relaxation curves agree very well with those of the experimental ones. The three-dimensional form predicted a slightly faster relaxation rate because the theoretical calculations were based on a slightly faster rate of strain. Both experimental and theoretical values show that the course of the stress-relaxation became independent of initial stretching history after 600 s beyond which all curves merged into one.

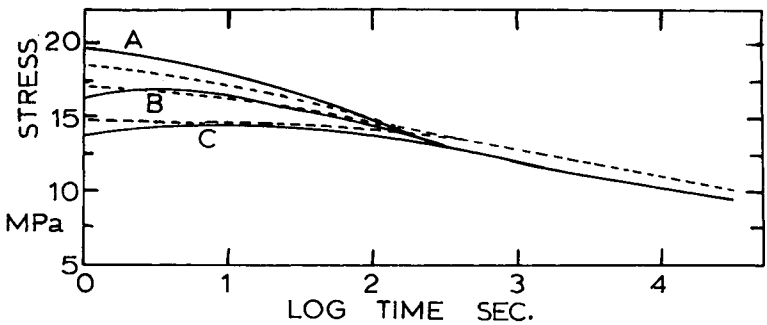

Fig. 13. Stress-relaxation data for high-density polyethylene at room temperature at initial strains (A) 0.065, (B) 0.01 and (C) 0.077 each reduced to 0.065 at the start of the test. Solid lines, data replotted from Shinozaki and Sargent[21] and dashed lines calculated using the parameters based on $n = 7$ with $R = 2.08 \times 10^{-2}$ MPa^{-1}, $B = 8.38 \times 10^{-1}$ MPa^{-1}, $G_1 = 161.9$ MPa and $G_2 = 41.4$ MPa.

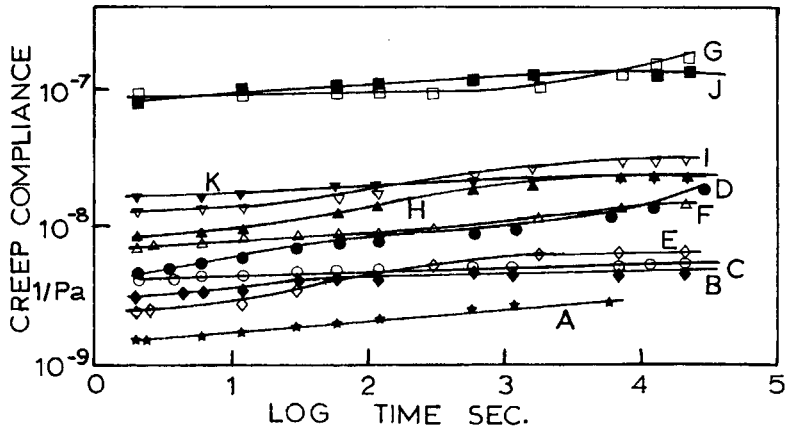

Fig. 14. Creep compliance versus time at 295 K. Initial stress is reached at a strain rate of 6.67 h^{-1}. Initial stresses were (A) 4GT 50.2 MPa, (B) 6GT 22.3 MPa, (C) 8GT 20.9 MPa, (D) 10GT 18.8 MPa, (E) 4GI 27.0 MPa, (F) 6GI 14.7 MPa, (G) 10GI 2.9 MPa, (H) 3GTcoI 17.1 MPa, (I) 4GTcoI 18.1 MPa, (J) 6GTcoI 4.8 MPa, (K) 10GTcoI 8.7 MPa.

More recently,[22] various linear aliphatic nylons were studied and the stress-relaxation could be predicted well using the three-dimensional equations.

Prediction of Creep

The experimental creep curve of 4GTcoI was compared with the theoretical creep curves with $a = 10$, 5, -0.1, and -0.8. There was no significant difference between the two calculated curves with $a = -0.1$ and -0.8. However, as the value of a increased from 5 to 10, the theory predicted a larger initial elongation followed by a slower creep rate. All the theoretical curves converged to the same asymptotic value at longer times. The predictions of the model, with the exception of $a = 10$, compared favorably with the experimental creep data.

The results of creep experiments for eleven aromatic polyesters tested at 295 K are shown in Figure 14. The strain history of the specimens prior to each creep test is given in Table III. The creep compliance is the time-dependent quotient of $\epsilon(t)/\sigma_0$. The curves are compiled in the same diagram by choosing initial stresses σ_0 of comparable values. Figure 14 shows that the creep rate at short time is more or less the same for all materials tested. As the amount of deformation increases with time, viscous phenomena become increasingly important. Samples 10GT and 10GI showed some signs of necking or rapid viscous deformation after a duration of about 1 h. Sample 4GT developed a crack followed by brittle fracture after a creep test of about 2 h.

Figure 15 shows the experimental creep data and the corresponding theoretical predictions for the terephthalate series. The three-dimensional predictions are in good qualitative agreement with the experimental creep results of 4GT, 6GT, and 8GT. This is not the case for 10GT for which the experimental values show a larger initial strain followed by a slower creep rate. The theoretical curve of the three-dimensional approach predicted a much smaller initial strain with a rapid rate of deformation. This prediction for 10GT is regarded as extremely poor. The one-dimensional equation predictions are also

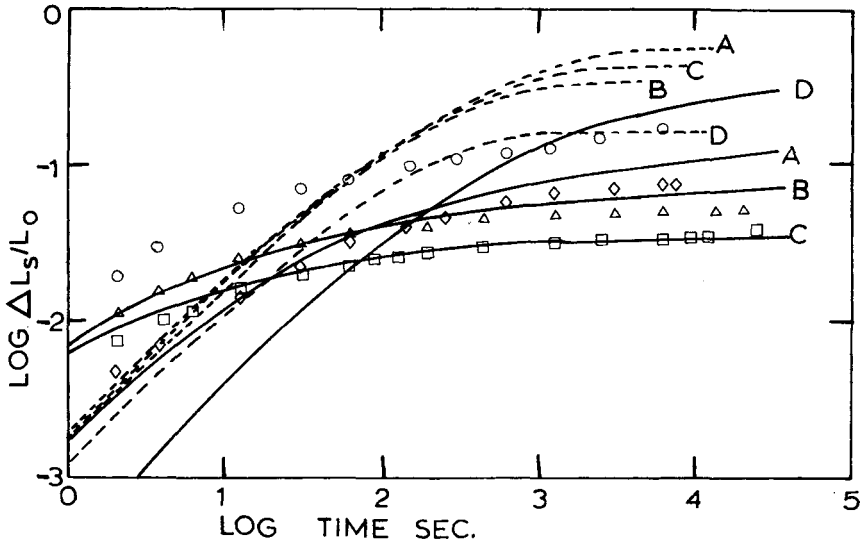

Fig. 15. Creep data for the terephthalate series for (A) 4GT at initial stress 50.2 MPa; (B) 6GT at initial stress 22.3 MPa; (C) 8GT at initial stress 20.9 MPa; and (D) 10GT at initial stress 18.8 MPa. Dashed lines are one-dimensional prediction, solid lines are three-dimensional predictions. (Parameters from Table I.)

considered very poor. Irrespective of the differences in the initial stresses σ_0, the creep curves obtained by the one-dimensional calculations for 4GT, 6GT and 8GT almost coincide with one another. This calculation predicted a strain of about 0.3 within 1 h of creep time making it unrealistic.

Figure 16 compares qualitatively the experimental and the theoretical behavior of the isophthalate series during creep tests. The theoretical predict-

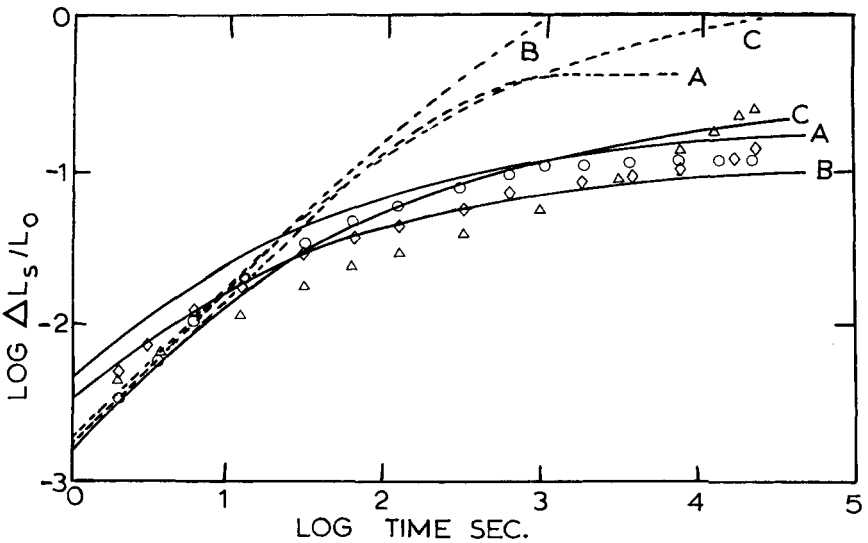

Fig. 16. Creep data for the isophthalate series for (A) 4GI at initial stress 27.0 MPa, (B) 6GI at initial stress 14.8 MPa and (C) 10GI at initial stress 2.9 MPa. Dashed lines are for one-dimensional and solid lines for three-dimensional equations. (Parameters from Table I.)

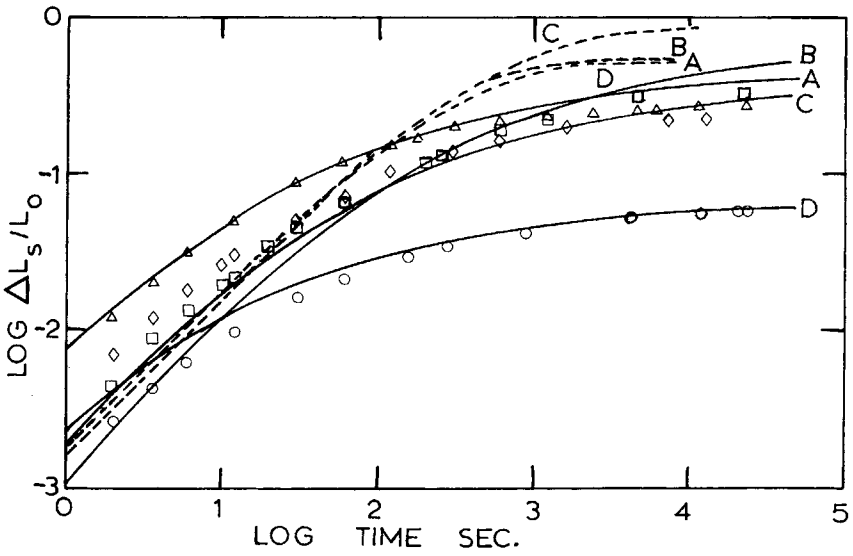

Fig. 17. Creep data for copolyester series for (A) 3GTcoI at initial stress 17.1 MPa, (B) 4GTcoI at initial stress 18.2 MPa, (C) 6GTcoI at initial stress 4.8 MPa and (D) 10GTcoI with initial stress 8.7 MPa. Dashed lines are for one-dimensional and solid lines for three-dimensional equations. (Parameters from Table I.)

ion based on three-dimensional calculations for the creep curve of 10GI does not fit the data sufficiently well. Sample 10GI exhibited necking after about 1 h of creep test. This phenomenon is associated with the stress concentration around the area of necking and resulted in a faster rate of elongation. The predictions based on the three-dimensional approach are in fair agreement with the data for 4GI and 6GI. Extremely poor agreement is obtained for the one-dimensional equation predictions.

The experimental creep data and the theoretical curves for the copolyester series are shown in Figure 17. Three-dimensional equation predictions are fair while the one-dimensional equation predictions are rather poor. The creep data of 10GTcoI were compared at three different stress levels; one below the yield point, the other two above it. The creep behavior above the yield point (σ_0 = 7.7 MPa and 8.7 MPa) is abnormal; the creep curve at σ_0 = 7.7 MPa is higher than that at σ_0 = 8.7 MPa. This can be explained by the fact that at the higher stress level, the specimen had been strained to a relatively higher initial strain such that the subsequent elongation was less than that at σ_0 = 7.7 MPa. The three-dimensional equations failed to predict such an observation.

SUMMARY

One-dimensional equations and three-dimensional equations based on the Halsey-Eyring three element model were used to predict stress relaxation and creep from constants measured on a stress-strain curve of the same materials. The one-dimensional equations failed to predict stress relaxation and creep in the nonlinear viscoelastic region. The three-dimensional equations use stress and rate of strain tensors. The result is still a simple model which describes

such features of the viscoelastic behavior as stress-relaxation and creep quite well.

The time derivative of the stress tensor used in the three-dimensional approach produces an expression containing a constant a. The study shows that with a between -1 and 1 does not change its predicting power appreciably. Although the values of a between 5 and 10 shift the theoretical curves a great deal, there is no guarantee that the qualitative predictions are improved.

The three-dimensional equations with $\eta\alpha \exp(-B|\tau_1|)$ predicts the stress-relaxation data more satisfactorily at moderate strain levels near the yield point while that with $\eta\alpha|\tau_1|\exp(-B|\tau_1|)$ makes better stress-relaxation predictions at strain levels much higher than the yield strain.

The stress-relaxation data on high-density polyethylene and on linear aliphatic polyamides in the literature were predicted by the three-dimensional equations with good agreement with experiment.

Supported by the Natural Sciences and Engineering Research Council of Canada.

References

1. H. Eyring and G. Halsey, *Text. Res. J.*, **16**, 6 (1946).
2. H. Eyring, *Rayon Tex. Mon.*, **71**, 519 (1945).
3. H. Eyring and G. Halsey, *High Polymer Physics*, A. A. Robinson, Ed., Chemical Publishing Co., New York, 1948.
4. H. Eyring, *J. Chem. Phys.*, **4**, 283 (1936).
5. R. N. Haward and G. Thackray, *Proc. Roy. Soc. London, A*, **302**, 453 (1968).
6. G. Titomanlio and G. Rizzo, *Proc. 7th Intl. Congr. Rheol., Gothenburg, Sweden, Aug. 23–27*, Swedish Society of Rheology, c/o Department of Polymeric Materials, Chalmers University of Technology, Gothenburg, Sweden, 1976, p. 522.
7. G. Titomanlio and G. Rizzo, *Polym. Eng. Sci.*, **18**, 767 (1978).
8. A. K. Doolittle, *J. Appl. Phys.*, **22**, 1471 (1951).
9. J. G. Oldroyd, *Proc. Roy. Soc. London, A*, **245**, 278 (1958).
10. T. H. Ng, *Study of Stress-Strain-Time Relationship of Linear Aromatic Polyesters in the Nonlinear Viscoelastic Region*, University of Toronto, Toronto, Canada (1983). NLC *Diss. Abstr. Intl. B.*, **45(2)**, 640 (1984), cf *C.A.*, **101**, 152657m (1984).
11. T. H. Ng and H. Leverne Williams, *Makromol. Chem.*, **182**, 3323, 3331 (1981).
12. T. H. Ng and H. Leverne Williams, *J. Appl. Polym. Sci.*, **32**, 4883 (1986).
13. G. V. Vinogradov and A. Ya. Malkin, *Rheology of Polymers*, Mir. Pub., Moscow, 1980, p. 130.
14. A. S. Krauz and H. Eyring, *Deformation Kinetics*, Wiley-Interscience, New York, 1975, p. 38.
15. S. L. Rosen, *Fundamental Principles of Polymer Materials for Practising Engineers*, Barnes & Noble, Inc., New York, 1971, p. 198.
16. G. Astarita and G. Marrucci, *Principles of Non-Newtonian Fluid Mechanics*, McGraw-Hill, London, 1974, pp. 18, 216.
17. G. Titomanlio and G. Rizzo, *J. Appl. Polym. Sci.*, **21**, 2933 (1977).
18. T. L. Smith, *J. Polym. Sci.*, **17**, 2181 (1978).
19. J. Meissner, *J. Polym. Sci.*, **16**, 915 (1978).
20. J. D. Ferry, *Viscoelastic Properties of Polymers*, Wiley, New York, 1980, p. 292.
21. D. M. Shinozaki and C. M. Sargent, *Material Sci. Eng.*, **35**, 213 (1978).
22. W. V. Bradley and H. Leverne Williams, *J. Appl. Polym. Sci.*, **32**, 2889 (1986).

Received January 31, 1985
Accepted June 6, 1986